

The effect of thresholding on temporal avalanche statistics

Lasse Laurson, Xavier Illa, and Mikko J. Alava

Department of Applied Physics, Helsinki University of Technology, FIN-02015 HUT, Finland

E-mail: `firstname.lastname (at) tkk.fi`

Abstract. We discuss intermittent time series consisting of discrete bursts or avalanches separated by waiting or silent times. The short time correlations can be understood to follow from the properties of individual avalanches, while longer time correlations often present in such signals reflect correlations between triggerings of different avalanches. As one possible source of the latter kind of correlations in experimental time series, we consider the effect of a finite detection threshold, due to e.g. experimental noise that needs to be removed. To this end, we study a simple toy model of an avalanche, a random walk returning to the origin or a Brownian bridge, in the presence and absence of superimposed delta-correlated noise. We discuss the properties after thresholding of artificial timeseries obtained by mixing toy avalanches and waiting times from a Poisson process. Most of the resulting scalings for individual avalanches and the composite timeseries can be understood via random walk theory, except for the waiting time distributions when strong additional noise is added. Then, to compare with a more complicated case we study the Manna sandpile model of self-organized criticality, where some further complications appear.

PACS numbers: 05.40.Fb, 45.70.Ht

1. Introduction

Many systems in Nature are characterized by an intermittent avalanche-like response to slow externally applied driving [1]. Examples range from laboratory scale experiments on magnetic systems [2] and e.g. the sound emitted in a fracture test on a piece of paper [3], to various applications in plasma physics and astrophysics [4, 5, 6], as well as in geophysics, including in particular earthquakes occurring due to the interaction of slowly moving tectonic plates [7]. Often the easiest way to characterize the dynamics of such systems is to record a *global* activity time series $V(t)$, such as the acoustic emission (AE) amplitude in the paper fracture experiment [3], the induced voltage in a Barkhausen noise measurement [2] or the AE activity in martensites [8]. Such signals are often observed to be composed of apparently distinct bursts or pulses, which in the limit of slow driving are associated to distinct and typically spatially localized avalanches of activity occurring in the system. A typical feature of such bursts or avalanches is that the statistics of various measures associated to them appear to lack a characteristic scale, e.g. the avalanche sizes and often also durations are usually characterized by power law distributions.

Another often made observation is that such avalanche-like signals appear to exhibit complex temporal correlations. On shorter time scales, the correlations can be thought to arise from individual avalanches, and a scaling theory relating the high frequency power spectra of such signals to the scaling properties of individual avalanches has been demonstrated to apply in a number of systems with avalanche dynamics [9, 10, 11, 12]. Longer time correlations are often assumed to be due to correlations between the triggerings of different avalanches. Such apparently distinct bursts of activity are often found to be clustered in time. In the context of earthquakes, events are usually divided into large main events with smaller fore- and aftershocks occurring before and after the main shock, respectively. The rate of aftershocks is typically found to obey Omori's law, i.e. it decays as a power law in time after the main shock [13]. Similar conclusions have been obtained for the foreshocks [14, 15].

Another possibility to detect correlations between different avalanches is to study the distributions of waiting times between two consecutive avalanches. If the avalanches are triggered by an uncorrelated process, one expects the waiting times to obey an exponential distribution due to the Poisson process -like random triggering of avalanches [16]. Consequently, deviations from this simple form can be interpreted to indicate the presence of correlations in the triggering process. In a number of systems, the distributions of waiting times between avalanches are found to be of power-law type [3, 17, 18, 19, 20, 21, 22].

Such correlations can have various origins depending on the physical situation at hand, and it is often difficult to identify the mechanism operating in a specific experiment. In systems where the avalanches are triggered by the external driving (as opposed to situations like thermal creep in which thermal fluctuations trigger the avalanches), numerical studies show that the inter-avalanche correlations can be due

to the properties of the driving signal [16, 23]. One must also be sure that a global activity signal is considered: In a *local* $V(t)$ -signal, non-exponential waiting times can be observed due to the spatiotemporal fractal nature of critical avalanches [24]. In general, one can define a probability per unit time that an avalanche is triggered somewhere in the system. If other mechanisms for the observed correlations such as those mentioned above can be excluded, a possibility is that the occurrence of an avalanche somehow intrinsically affects this probability, thus leading to inter-avalanche correlations.

In this paper we will focus on the effect of a finite detection threshold necessarily present in any real experimental situation. The presence of a background, either due to noise or processes coexisting with the intermittent avalanches in a measured activity time series $V(t)$, forces one to apply a finite threshold level V_{th} , and define avalanches as the bursts exceeding this threshold [11, 12]. While such ideas have attracted some attention in the literature [25, 26, 27], neither theoretically nor experimentally general studies have been carried out on the effect of thresholding on the avalanche statistics. Since an avalanche can be defined as a correlated sequence of activity, breaking the avalanche into smaller parts by thresholding, the ensuing “subavalanches” will be temporally correlated, being part of the same underlying avalanche. As an attempt to clarify the issues associated to this effect of thresholding, we consider a simple toy model of the signal $V(t)$ corresponding to a single avalanche, namely an excursion of a random walk from the origin. Such a simple model is sufficient to demonstrate how e.g. the distribution of waiting times arising from the thresholding process assumes a power law form. We also discuss the same phenomenology in the stochastic Manna sandpile model of self-organized criticality [29]. We also consider the addition of external noise, and the properties of composite signals made of toy avalanches and waiting times from a distribution chosen a priori: how thresholding affects them with or without the noise. For avalanche sizes and power spectra, there are no real complications, but for the waiting times we find a mixture of effects including an apparent power-law regime with a different exponent, when noise is added. The paper is organized as follows: In the next Section, excursions of random walks as a model of an avalanche signal is considered. The Manna sandpile model is briefly discussed in Section 3. Section 4 finishes the paper with conclusions and a summary of future prospects.

2. The random walk model

As a conveniently simple toy model illustrating the mechanisms associated to the thresholding process of avalanche time series, we consider an excursion of a discrete random walk, obeying

$$\partial_t x = \eta, \tag{1}$$

where η is white noise with a bimodal distribution $P(\eta) = 1/2(\delta_{\eta,1} + \delta_{\eta,-1})$ and time is updated in steps of magnitude $\Delta t = 1$. The excursion starts at $t = 0$ from $x = 0$, and returns to the origin for the first time at $t = T$. Such a random walk bridge is then taken to model the $V(t)$ -signal corresponding to a single avalanche of duration T .

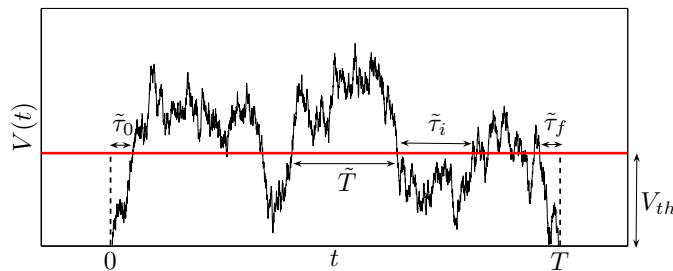


Figure 1. An example of subavalanches obtained when a random walk bridge of given duration T is thresholded with a threshold level V_{th} , with the definitions of the different waiting times (or quiet times) $\tilde{\tau}_0$, $\tilde{\tau}_i$ and $\tilde{\tau}_f$.

The statistical properties of such excursions are well known [31, 32, 33]. The first return times, or avalanche durations T obey a power law distribution

$$P(T) \sim T^{-\tau_T} \quad (2)$$

for $T \gg 1$, with $\tau_T = 3/2$. Similarly, the distribution of avalanche sizes $s = \int_0^T V(t)dt$ is given by

$$P(s) \sim s^{-\tau_s}, \quad (3)$$

with $\tau_s = 4/3$. The average shape of the excursion is given by a semicircle,

$$V(t, T) = T^{\gamma_{st}-1} f_{shape}(t/T), \quad (4)$$

where $f_{shape}(x) = \sqrt{8/\pi} \sqrt{x(1-x)}$ and $\gamma_{st} = 3/2$. The exponent γ_{st} relates the average avalanche size, $\langle s(T) \rangle = \langle \int_0^T V(t)dt \rangle$ to the duration T as $\langle s(T) \rangle \sim T^{\gamma_{st}}$.

2.1. Random walk bridges of a given duration

First we will focus on the statistical properties of the avalanches which emerge when random walk bridges of fixed duration T are thresholded as is showed if Fig. 1.

The first quantity of interest is the number of avalanches $N(T, V_{th})$ as a function of the random walk bridge duration T and the threshold level V_{th} . The upper panel of Fig. 2 shows the number avalanches observed as a function of the threshold level V_{th} , for various durations T of the unthresholded excursions. These can be collapsed onto a single curve by using the ansatz

$$N(T, V_{th}) = T^\alpha f_N(V_{th}/T^{1/2}). \quad (5)$$

The value of the exponent $\alpha = 0.51 \pm 0.01$ is observed to be close to $1/2$, a result that can be understood to follow from the known scaling of the number of zero crossings $N_{zc}(t)$ of a random walk as a function of time, $N_{zc}(t) \sim t^{1/2}$ [33].

The lower panel of Fig. 2 displays the distributions of the maxima of the random walk excursions. Again, a good data collapse is obtained by using the scaling

$$P(x_{max}, T) = T^{-1/2} f_{x_{max}}(x_{max}/T^{1/2}), \quad (6)$$

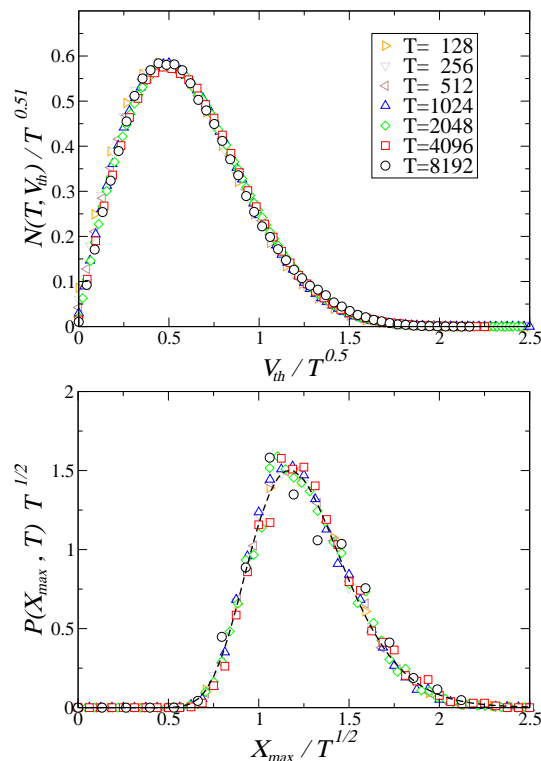


Figure 2. Top: The rescaled number of waiting times as a function of the threshold level V_{th} , for different avalanche durations T . Bottom: The rescaled distributions of the maximum values of the avalanche signal as a function of threshold level V_{th} , for different avalanche durations T . The dashed line is a fit to a log-normal distribution $f(x; \mu, \sigma) = [1/(x\sigma\sqrt{2\pi})] \exp(-(\log(x) - \mu)^2/(2\sigma^2))$, with $\mu = 0.21$ and $\sigma = 0.22$.

with an apparently universal scaling function $f_{x_{max}}(y)$ that can be fitted well with a log-normal distribution. The two first moments of this fitted distribution are in agreement with the ones computed in Ref. [28] using the exact expression.

When a non-zero threshold V_{th} is applied, one can define three different kinds of waiting times: the initial waiting time $\tilde{\tau}_0$, the intra-avalanche waiting times $\tilde{\tau}_i$, and the final waiting time $\tilde{\tau}_f$, see Fig. 1. Notice that in this paper we denote all quantities x defined with a non-zero threshold level V_{th} like \tilde{x} , while x stands for the same thing with $V_{th} = 0$. Since for models with a symmetrical avalanche shape $P(\tilde{\tau}_f; T, V_{th}) = P(\tilde{\tau}_0; T, V_{th})$, we focus on the distributions of $\tilde{\tau}_0$ and $\tilde{\tau}_i$. The former one can be collapsed using the scaling ansatz

$$P(\tilde{\tau}_0; T, V_{th}) \sim V_{th}^{-2} g(\tilde{\tau}_0/V_{th}^2). \quad (7)$$

Due to the Markovian and translation invariance properties of the random walk, $P(\tilde{\tau}_i; T, V_{th})$ is expected to be of a power law form with the same exponent as $P(T)$ (as $\tilde{\tau}_i$'s are just the durations of the excursions below the threshold V_{th}), i.e.

$$P(\tilde{\tau}_i; T, V_{th}) \sim \tilde{\tau}_i^{-3/2} f(\tilde{\tau}_i/V_{th}^2) f_T(\tilde{\tau}_i/T). \quad (8)$$

The cut-off scaling follows from the restriction that such excursions below the threshold

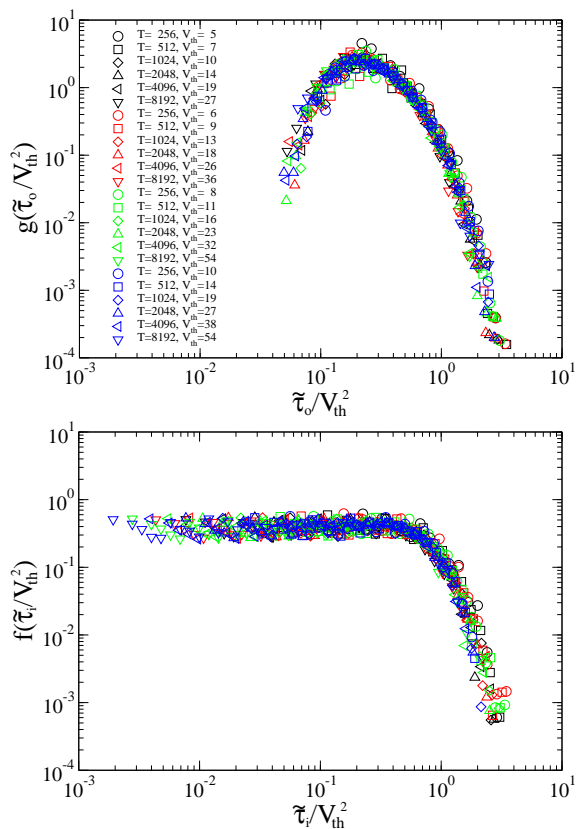


Figure 3. Scaling functions for the initial waiting time distribution (top) and for the intra-avalanche waiting time distribution (bottom). Different colours (online version) account for different values of $r = V_{th}/T^{1/2} = 0.3, 0.4, 0.5, 0.6$. For larger r -values the intra-avalanche waiting times $\tilde{\tau}_i$ do not obey Eq. (9) as for very large r the cut-off due to the finite avalanche duration becomes important, see Eq. (8).

are bounded between 0 and V_{th} , so that a maximum waiting time scaling as V_{th}^2 ensues, see Eq. (4). For random walk bridges of a fixed duration T , another constraint is that $\tilde{\tau}_i < T$. However, in practice the cut-off scale due to the finite threshold value is reached first, and the scaling function $f_T(x)$ can be regarded as a constant. Thus, one can write a T -independent form for the distribution of internal waiting times,

$$P(\tilde{\tau}_i; T, V_{th}) \sim P(\tilde{\tau}_i; V_{th}) \sim \tilde{\tau}_i^{-3/2} f(\tilde{\tau}_i/V_{th}^2). \quad (9)$$

Fig. 3 displays data collapses of distributions of $\tilde{\tau}_0$ and $\tilde{\tau}_i$. The intra-avalanche waiting times $\tilde{\tau}_i$ obey Eq. (9) only for $r < 0.7$ as for very large r the cut-off due to the finite avalanche duration becomes important, see Eq. (8).

Next we consider both the initial and the internal waiting times together, by defining $\tilde{\tau} = \tilde{\tau}_0 \cup \tilde{\tau}_i$. The total distribution of waiting times $\tilde{\tau}$ is then given by

$$P(\tilde{\tau}; T, V_{th}) = \frac{P(\tilde{\tau}_0; T, V_{th}) + (N(T, V_{th}) - 1)P(\tilde{\tau}_i; T, V_{th})}{N(T, V_{th})}. \quad (10)$$

For $T \gg 1$, the number of subavalanches $N(T, V_{th}) \gg 1$, see Eq. (5) and Fig. 2. In this limit $N(T, V_{th}) - 1 \simeq N(T, V_{th})$ and one obtains the total distribution of waiting times

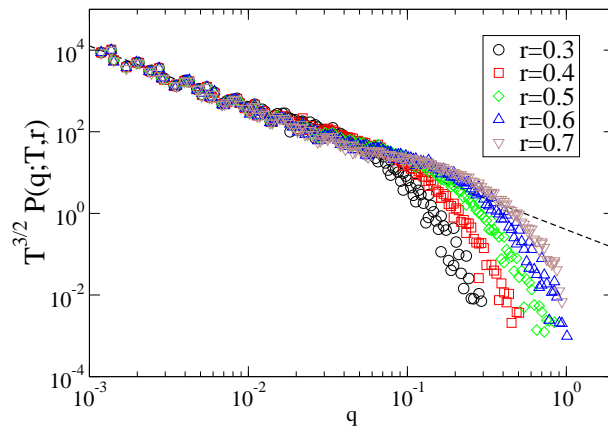


Figure 4. Scaling functions for the total waiting time distribution for different values of r .

for a fixed duration T and threshold level V_{th} :

$$P(\tilde{\tau}; T, V_{th}) = V_{th}^{-2} \frac{g(\tilde{\tau}/V_{th}^2)}{f_N(V_{th}/T^{1/2})} T^{-\alpha} + \tilde{\tau}^{-3/2} f(\tilde{\tau}/V_{th}^2). \quad (11)$$

Now, using the more natural variables $r = \frac{V_{th}}{T^{1/2}}$ and $q = \frac{\tilde{\tau}}{T}$, one can rewrite the above equation as

$$P(q; T, r) = T^{-3/2} \left[\frac{g(q/r^2)}{r^2 f_N(r)} + q^{-3/2} f(q/r^2) \right], \quad (12)$$

which allows us to collapse the total waiting time distributions for a given value of r for all durations T , as can be seen in Fig. 4. Moreover, the use of these variables also allows us to write the mean value of the total waiting time distribution as

$$\langle \tilde{\tau} \rangle = T^{1/2} \left[I_1 \frac{r^2}{f_N(r)} + I_2 r \right], \quad (13)$$

where $I_1 = \int d\xi \xi g(\xi)$ and $I_2 = \int d\xi \xi^{-1/2} f(\xi)$.

2.2. Entire signal

In order to generate an artificial signal, one can insert exponentially distributed waiting times (corresponding to uncorrelated triggerings of the avalanches) between the original (non-thresholded) avalanches and study the evolution of the waiting time distribution as the threshold level V_{th} is increased from zero as can be seen in Fig. 5 (top). Also the effect of adding white noise to the random walk signal is considered as can be seen in Fig. 5 (bottom).

The total statistics arising from the intra-avalanche properties of an ensemble of excursions with duration distribution given by Eq. (2) at a fixed threshold is obtained as a convolution over $P(T)$. For instance, one can write for the distribution of internal waiting times

$$P(\tilde{\tau}_i; V_{th}) = \int P(T) P(\tilde{\tau}_i; T, V_{th}) dT \sim \tilde{\tau}_i^{-3/2} f(\tilde{\tau}_i/V_{th}^2), \quad (14)$$

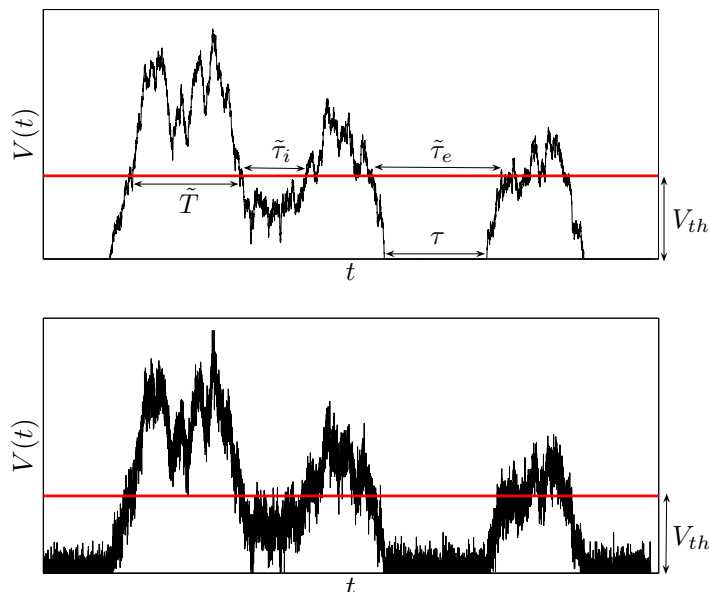


Figure 5. Top: An example of a signal $V(t)$ consisting of two random walk excursions from the origin, showing the definitions of the avalanche duration \tilde{T} and the waiting times (or quiet times) $\tilde{\tau}$ after thresholding the signal with a threshold level V_{th} indicated in the figure by the horizontal line. Bottom: The same signal as above, but with superimposed Gaussian white noise. The presence of noise forces one to apply a finite threshold, but affects also the thresholded avalanches.

where the last step follows from the fact that $P(\tilde{\tau}_i; V_{th}, T)$ is independent of T . Similar considerations apply for the duration and size distributions of the subavalanches induced by the thresholding process, such that the thresholded avalanche durations \tilde{T} obey $P(\tilde{T}) \sim \tilde{T}^{-3/2}$. Similarly, thresholded avalanche sizes $\tilde{s} = \int_0^{\tilde{T}} [V(t) - V_{th}] dt$ follow the scaling $P(\tilde{s}) \sim \tilde{s}^{-4/3}$, see Fig. 6.

When considering the case with exponentially distributed waiting times τ inserted between subsequent random walk excursions, and studying the distributions of all waiting times $\tilde{\tau} = \tilde{\tau}_i \cup \tilde{\tau}_e$ (see Fig. 5) as a function of the applied threshold V_{th} , an evolution from an exponential to a power law distribution is observed as the threshold V_{th} is increased, see Fig. 7.

From an experimental point of view, all $V(t)$ -signals are noisy. In order to treat these real signals, one should add a minimum threshold to get rid of the background noise but keeping the maximum amount of information. Therefore, to study this effect in our artificial signals, we add a Gaussian white noise ξ with mean zero and standard deviation σ to the $V(t)$ -signal and consider different thresholds ranging from $V_{th} = 4\sigma$ to $V_{th} = 8\sigma$. Surprisingly, the exponent appears to change from $\tau_w = 3/2$ to $\tau_w \approx 2$, see Fig. 8. This change is because the original (without noise) waiting times are broken into shorter ones by the noise, but we have not managed yet to find a mathematical derivation of such an exponent.

These results demonstrate how a symmetry between the avalanche durations and

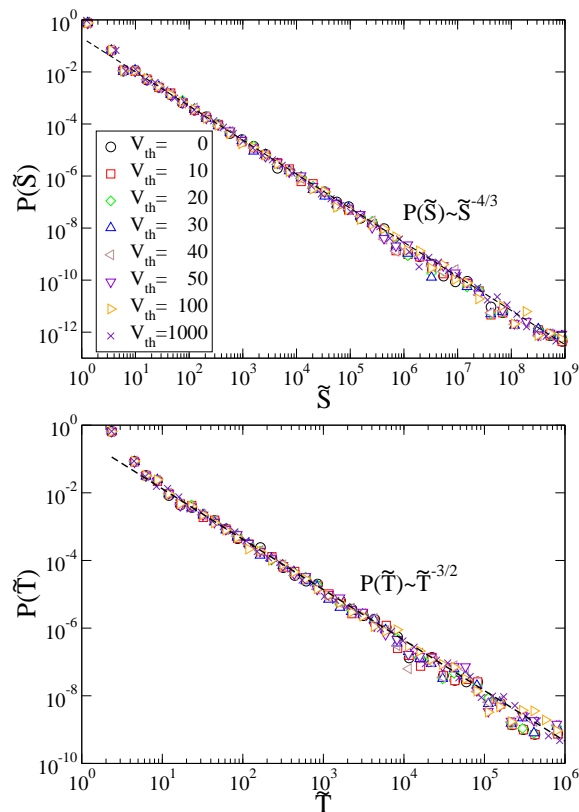


Figure 6. The probability distributions of avalanche sizes \tilde{s} (top) and durations \tilde{T} (bottom) for different threshold levels V_{th} .

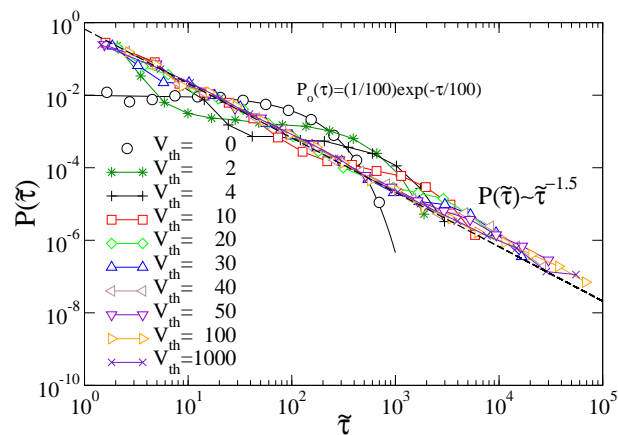


Figure 7. The probability distributions of waiting times (or quiet times) $\tilde{\tau} = \tilde{\tau}_i \cup \tilde{\tau}_e$ (see Fig. 5) between avalanches, for different threshold values, and waiting times between the non-thresholded excursions drawn from a probability distribution $P_o(\tau) = (1/b)\exp(-\tau/b)$, with $b = 100$. For $V_{th} = 0$ one recovers the exponential $P_o(\tau)$ distribution, while for large enough threshold values the distributions become power laws with an exponent $\tau_w \approx 1.5$.

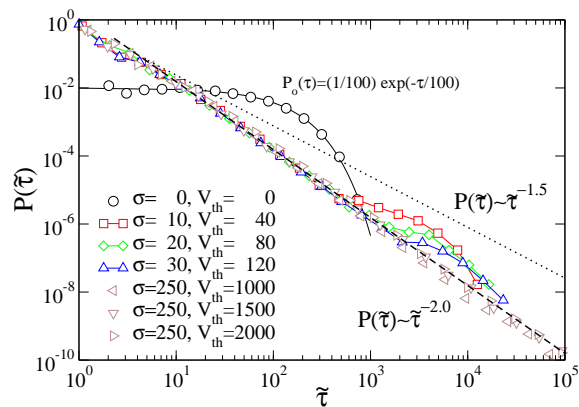


Figure 8. The probability distributions of waiting times (or quiet times) $\tilde{\tau}$ between avalanches with additive Gaussian white noise, for different threshold values V_{th} and noise strengths σ . The waiting times between the non-thresholded excursions drawn from a probability distribution $P_0(\tau)$. The power law exponent τ_w changes from the noise free value of $\tau_w = 3/2$ to $\tau_w \approx 2.0$. Considering the same signal *without* the artificial waiting times (not shown) produces similar distributions, with the only difference being a decrease in the magnitude of the “bump” in the cut-off due to the artificial waiting times.

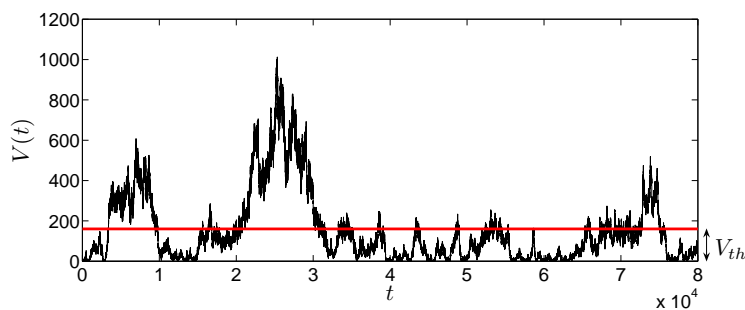


Figure 9. An example of a signal $V(t)$ consisting of avalanches from the 2d Manna model with $L = 1024$. The horizontal line corresponds to a threshold level with $V_{th} = 160$.

quiet time intervals could give a natural explanation to observations of power law distributed waiting times in various experimental situations in which any kind of thresholding process is applied. To see how such considerations can be generalized to more realistic systems with non-trivial dynamics, we consider in the following the same phenomenology in the two-dimensional stochastic Manna sandpile model of self-organized criticality.

3. Manna model

Out of many possible model systems, we consider here the Manna sandpile model of self-organized criticality [29]. This stochastic model has the advantage over some other models that it is known to obey simple scaling, whereas models such as the

original sandpile model introduced by Bak, Tang and Wiesenfeld (BTW) [30] has been observed to exhibit multiscaling [34]. In Ref. [26], the effect of thresholding on the statistics of quiet time intervals and avalanche durations was considered. Similarly to our observations above concerning the simple random walk model, the exponents describing the distributions of the avalanche durations and quiet time intervals were observed to be the same, but with a value close to $5/3$, different from both the random walk value of $3/2$ and the value found for the avalanche durations in the BTW model *without* thresholding [35]. One should notice, however, that the latter observations regarding the exponent values can be masked by the multiscaling exhibited by the BTW model [34].

The stochastic Manna model is defined on a d -dimensional hypercubic lattice of a linear size L , with an integer variable z_i assigned to each lattice site i . A site *topples* if the local variable reaches or exceeds a critical value $z_c = 2$. In the toppling process, two grains will be redistributed from the toppling site to its two randomly chosen nearest neighbours. During a single time step, all the sites will be checked and those with $z_i \geq z_c = 2$ will be toppled in parallel. Such a toppling can then cause one of the neighbouring sites of the toppling site to topple during the next time step. Thus, an avalanche of activity can be triggered from a single initial toppling event. Such triggerings happen due to the addition of new grains to random locations in the system at a slow rate. This external driving is balanced by allowing grains to leave the system through the open boundaries. This combination of slow driving and dissipation drives the system to the critical point of an underlying absorbing phase transition, taking place at a critical value ξ_c of the grain density $\xi = N/L^d$ [36, 37].

Here, we consider the two dimensional version of the model, and study the time series $V(t)$ measuring the number of toppling events as a function of time, with one parallel update of the lattice defining the unit of time. Fig. 9 shows an example of a time series $V(t)$ from the $2d$ Manna model with $L = 1024$. By driving the system with a slow constant rate, the waiting times between avalanches without any thresholding will follow exponential statistics. The non-thresholded avalanche durations are distributed according to a power law with an exponent $\tau_T \approx 1.5$. The average avalanche size $\langle s(T) \rangle$ scales with the avalanche duration as $\langle s(T) \rangle \sim T^{\gamma_{st}}$, with $\gamma_{st} \approx 1.77$ [10]. As the threshold level V_{th} is increased from zero, a power law part starts to emerge to the internal waiting time distribution, with a cut-off $\tilde{\tau}_i^*$ scaling roughly as

$$\tilde{\tau}_i^* \sim V_{th}^{1/(\gamma_{st}-1)} \approx V_{th}^{1.3}, \quad (15)$$

The exponent τ_w assumes a value close to the one observed for the BTW model [26], i.e. $\tau_w \approx 1.62 \pm 0.05$, see Fig. 10. Similar power law scaling is observed by considering the ensemble of all waiting times, $\tilde{\tau} = \tilde{\tau}_e \cup \tilde{\tau}_i$, where $\tilde{\tau}_e$ denotes the inter-avalanche waiting times. The power law exponent remains unchanged from the case where only $\tilde{\tau}_i$'s are considered, but the inclusion of $\tilde{\tau}_e$'s has the effect of producing a ‘‘bump’’-like cut-off to the distributions. Interestingly, Fig. 11 shows that also the duration distribution exponent appears to evolve towards a similar value as the threshold level V_{th} is increased, in agreement with the observations in the BTW model [26].

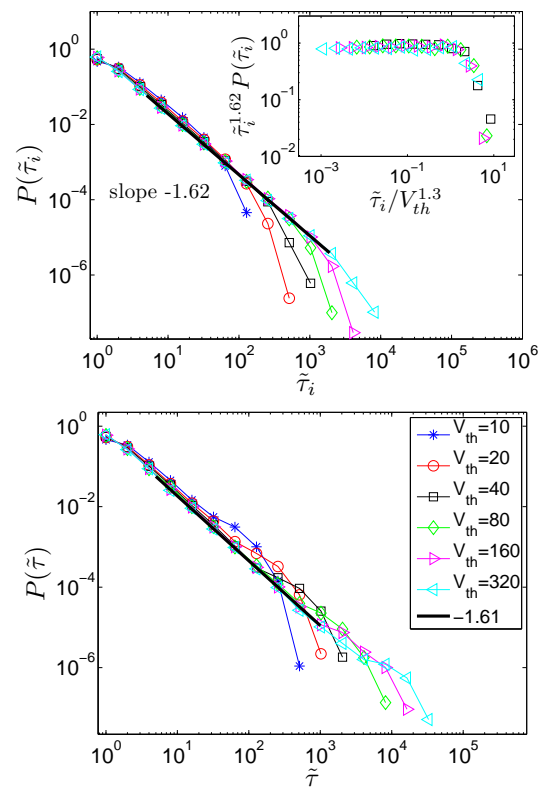


Figure 10. Top: The distributions of the intra-avalanche waiting times $\tilde{\tau}_i$ in the $d = 2$ Manna model with $L = 1024$ as a function of the threshold level V_{th} . The solid line corresponds to a power law with an exponent $\tau_w = 1.62$. The inset displays a data collapse of the distributions for $V_{th} \geq 40$ showing that the cut-off scales as $\tilde{\tau}_0^* \sim V_{th}^{1.3}$. Bottom: The distributions of all (intra-avalanche as well as inter-avalanche) waiting times $\tilde{\tau}$. The solid line corresponds to a power law with an exponent $\tau_w = 1.61$.

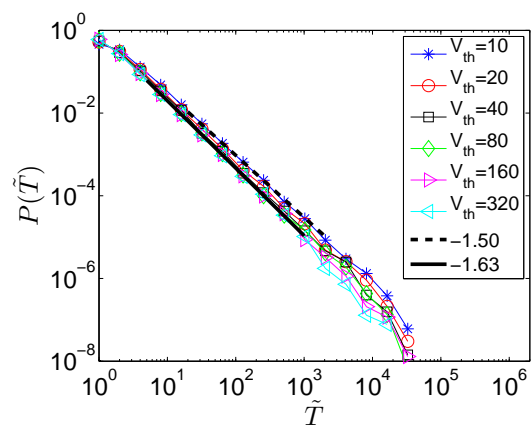


Figure 11. The distributions of avalanche durations \tilde{T} in the $d = 2$ Manna model with $L = 1024$ as a function of the threshold level V_{th} . The exponent τ_T appears to evolve from 1.5 to 1.63 as the threshold V_{th} is increased.

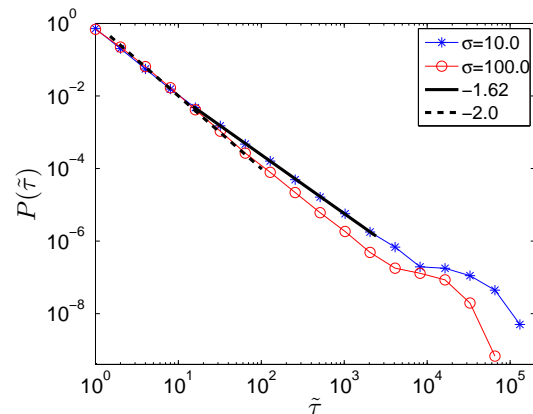


Figure 12. The distributions of waiting times $\tilde{\tau}$ in the $d = 2$ Manna model with $L = 1024$ and $V_{th} = 640$, for two different strengths σ of the additive Gaussian white noise. The exponent τ_w appears to change to $\tau_w \approx 2.0$ for short waiting times, while for waiting times longer than a σ -dependent crossover scale, the noise free value $\tau_w \approx 1.62$ persists.

Finally, we consider the effect of noise on the observed waiting time statistics in the Manna model. By adding Gaussian white noise with zero mean and standard deviation σ to the $V(t)$ -signal, we observe a similar change in the τ_w -exponent as in the case of the simple random walk model: it assumes a value close to $\tau_w \approx 2$ for waiting times smaller than some crossover scale growing with σ . For longer waiting times, the scaling is the same as in the absence of noise, $\tau_w \approx 1.65$, see Fig. 12.

4. Conclusions

The simple random walk model studied here presents a simple and transparent illustration of the mechanism leading to power law distributions of quiet times between consecutive subavalanches emerging from the thresholding process. A key observation here is that this can be understood to follow from the symmetry between the random walk excursions above and below the imposed threshold. The numerical result that such a symmetry appears to be valid also in the non-trivial case of the Manna sandpile model is an interesting observation that would deserve further attention. Also there is an apparent difference in the avalanche duration distribution exponents in the sandpile models between the unthresholded and thresholded cases, which is intriguing and not understood.

The other interesting observation is that additive Gaussian white noise can have an effect on the observed waiting time statistics. The apparent change in the power law exponent from the noise-free value to a value close to -2.0 both in the random walk and Manna models for high enough noise strength remains to be explained. This observation may be relevant when noisy experimental signals have to be thresholded.

Another technique that we have used to study the effect of thresholding on

these artificial signals is the Power Spectrum (PS) analysis. For the signal composed by random walk excursions the global behaviour of the PS does not change when thresholding due to the RW translational invariance, obtaining $P(f) = A/f^2$. The constant A is decreasing when the threshold is increased due to the fact that the total energy of the signal decreases. Similar observations, though less conclusive, can be obtained for the Manna model: the exponent of the power spectrum does not seem to change significantly from the non-thresholded case where $P(f) = A/f^\alpha$, with $\alpha = \gamma_{st} \approx 1.77$ [10]. The exponent γ_{st} is related to the avalanche distribution exponents through $\gamma_{st} = (\tau_T - 1)/(\tau_s - 1)$. As we observe an apparent change in the value of the τ_T -exponent, the τ_s -exponent should thus experience a corresponding change to keep γ_{st} constant. Given the above values for τ_T and γ_{st} , one would thus expect $\tau_s \approx 1.36$, to be compared with $\tau \approx 1.28$ for $V_{th} = 0$ [38]. However, due to the limited accuracy of the numerical values of these exponents, and to the small (if any) change to the PS exponent, we do not pursue this issue.

To discuss the implications of the toy models we have explored we note that power-law waiting times (and correlations) arise only after thresholding (single) avalanches. Then the self-affine character of the single avalanches produces power-law (PL) waiting times with a particular, model-dependent exponent. For empirical examples such as earthquakes the question is how to interpret the PL statistics and correlations in the cascades of aftershocks. Based on toy models one can envision three reasons for PL waiting times, or two additional ones beyond such thresholding. First, the system would be driven externally in a non-Poissonian way such that the PL statistics ensues. In the case of solar physics this has been argued to be the case for the magnetosphere, since it might be so that the solar wind which drives it has such correlations [39]. Second, the models we use could be far from the real dynamics, which may be much more complicated. We represent (in the Manna case, for instance) the dynamics with a projection to a one-dimensional signal $V(t)$, but in reality such a trick may produce a $V(t)$ that appears to have correlations among avalanches while in fact the system evolves dynamically also when $V(t)=0$. A similar mechanism would be that the system has a memory which e.g. is influenced by the size of an avalanche and influences the rate at which subsequent avalanches are triggered. The usual (e.g. SOC) models do not exhibit such, but this does not logically exclude the possibility at all.

Finally we point out that in addition to the temporal clustering of the avalanches, the effect of a finite detection threshold on the often observed *spatial* avalanche clustering could be considered as well. It is also intriguing as to what would happen to two-point correlations in spatio-temporal systems, in both time and space domains.

Acknowledgments

Most of this work has been done while visiting Nordita in Stockholm, and the authors wish to thank the institute for hospitality. LL acknowledges Satya Majumdar for interesting discussions regarding random walks. Academy of Finland is thanked for

financial support.

References

- [1] J. P. Sethna, K. A. Dahmen, and C. R. Myers, *Nature* **410**, 242 (2001).
- [2] G. Durin and S. Zapperi, *The Science of Hysteresis* ed. G. Bertotti and I. Mayergoyz (New York: Academic, 2005).
- [3] L. I. Salminen, A. I. Tolvanen, and M. J. Alava, *Phys. Rev. Lett.* **89**, 185503 (2002).
- [4] S. Chapman and N. Watkins, *Space Sci. Rev.* **95**, 293 (2001).
- [5] T. Chang, S. W. Y. Tam, C. C. Wu and O. Consolini, *Space Sci. Rev.* **107**, 425 (2003).
- [6] T. Chang, *Phys. Plasmas* **6**, 4137 (1999).
- [7] B. Gutenberg and C. F. Richter, *Seismicity of the Earth and Associated Phenomena* (Princeton Univ. Press, Princeton, 1954).
- [8] L. Carrillo, L. Mañosa, J. Ortín, A. Planes, and E. Vives, *Phys. Rev. Lett.* **81**, 1889 (1998).
- [9] M. C. Kuntz and J. P. Sethna, *Phys. Rev. B* **62**, 11699 (2000).
- [10] L. Laurson, M.J. Alava, and S. Zapperi, *J. Stat. Mech.: Theo. Exp.* 0511, L11001 (2005).
- [11] L. Laurson and M.J. Alava, *Phys. Rev. E* **74**, 066106 (2006).
- [12] M. Rost, L. Laurson, M. Dubé, and M.J. Alava, *Phys. Rev. Lett.* **98**, 054502 (2007).
- [13] F. Omori, *J. College Sci. Imper. Univ. Tokyo* **7**, 111 (1895).
- [14] B. C. Papazachos, *Bull. Seismol. Soc. Am.* **63**, 1973 (1973).
- [15] A. Helmstetter and D. Sornette, *J. Geophys. Res., [Solid Earth]* **B108**, 2457 (2003).
- [16] R. Sanchez, D. E. Newman, and B. A. Carreras, *Phys. Rev. Lett.* **88**, 068302 (2002).
- [17] J. Koivisto, J. Rosti, and M. J. Alava, *Phys. Rev. Lett.* **99**, 145504 (2007).
- [18] A. Corral, *Phys. Rev. Lett.* **92**, 108501 (2004).
- [19] R. D'Amicis, R. Bruno, B. Bavassano, V. Carbone, and L. Sorriso-Valvo, *Ann. Geophys.* **24**, 2735 (2006).
- [20] M. S. Wheatland and Y. E. Litvinenko, *Sol. Phys.* **211**, 255 (2002).
- [21] A. Guarino, S. Ciliberto, A. Garcimartin, M. Zei, R. Scorretti, *Eur. Phys. J. B* **26**, 141 (2002).
- [22] A. Corral, preprint submitted to this issue, arXiv:0809.4851.
- [23] M. Baiesi and C. Maes, *Europhys. Lett.* **75**, 413 (2006).
- [24] L. Laurson and M. J. Alava, *Eur. Phys. J. B* **42**, 407 (2004).
- [25] K. Christensen and Z. Olami, *J. Geophys. Res.* **97**, 8729 (1992).
- [26] M. Paczuski, S. Boettcher, and M. Baiesi, *Phys. Rev. Lett.* **95**, 181102 (2005).
- [27] M. Baiesi, M. Paczuski, and A. L. Stella, *Phys. Rev. Lett.* **96**, 051103 (2006).
- [28] S. N. Majumdar, J. Randon-Furling, M. J. Kearney, and M. Yor, *J. Phys. A: Math. Theor.* **41**, 365005 (2008).
- [29] S. S. Manna, *J. Phys. A: Math. Gen.* **24**, L363 (1991).
- [30] P. Bak, C. Tang, and K. Wiesenfeld, *Phys. Rev. Lett.* **59**, 381384 (1987).
- [31] S. Redner, *A Guide To First-Passage Processes* (Cambridge University Press, Cambridge, 2001).
- [32] F. Colaiori, A. Baldassarri, and C. Castellano, *Phys. Rev. E* **69**, 041105 (2004)
- [33] W. Feller, *Introduction to Probability Theory and Its Applications*, Vol. I, 3rd Edition (Wiley, 1968).
- [34] C. Tebaldi, M. De Menech, and A. L. Stella, *Phys. Rev. Lett.* **83** 3952 (1999).
- [35] S. Lübeck and K. D. Usadel, *Phys. Rev. E* **55**, 4095 (1997).
- [36] R. Dickman, M. A. Muñoz, A. Vespignani, and S. Zapperi, *Braz. J. Phys.* **30**, 27 (2000).
- [37] M. Alava, *J. Phys.: Condens. Matter* **14**, 2353 (2002).
- [38] S. Lübeck, *Int. J. Mod. Phys. B* **18**, 3977 (2004).
- [39] M. S. Wheatland, *Astrophys. J.* **536**, L109 (2000).